Effective medium for time-varying frequency-dispersive acoustic metamaterials

Xinghong Zhu,[1] Hong-Wei Wu,[2,*] Yue Zhuo,[2] Ziling Liu,[2] and Jensen Li[1,3,†]

[1]*Department of Physics, The Hong Kong University of Science and Technology, Clear Water Bay, Hong Kong, China*
[2]*School of Mechanics and Photoelectric Physics, Anhui University of Science and Technology, Huainan 232001, China*
[3]*William Mong Institute of Nano Science and Technology, Hong Kong University of Science and Technology, Hong Kong, China*

(Received 29 January 2023; accepted 17 August 2023; published 5 September 2023)

The effective medium theory is a key concept in metamaterials, with a growing interest in the temporal effective medium when the constitutive parameters are modulated with a period much shorter than the signal period. However, the effective medium with both frequency dispersion and time-varying resonating parameters is not clearly understood. In this work, we establish the temporal effective medium theory for acoustic metamaterials with time-varying frequency dispersion for compressibility. The formulas for the effective medium vary with the modulation of different resonance parameters and the transition from frequency-dispersive to -nondispersive regimes. Through experiments and theoretical models, we determine that time-varying resonance strength corresponds to the temporal average of compressibility β, time-varying resonating frequency corresponds to the temporal average of $1/(\beta–\beta_0)$ in the frequency-dispersive regime, and time-varying modulation amplitude in the nondispersive regime corresponds to the temporal average of $1/\beta$. These results clarify the effective medium for frequency-dispersive time-varying metamaterials and have potential applications in different classical waves such as acoustics, elastodynamics, and electromagnetism for designing temporal functional devices.

DOI: 10.1103/PhysRevB.108.104303

I. INTRODUCTION

Over the past two decades, metamaterials, which are constructed from subwavelength resonating structures arranged in periodic lattices, have proven to be a highly versatile platform for the realization of a wide range of counterintuitive phenomena [1–6]. Such phenomena include invisibility cloaks [7–9], mimicking gravitational lensing [10], and perfect lenses [11], among others. This versatility is made possible by the ability of metamaterials to produce effective medium parameters that are not attainable through conventional composite approaches. In order to enhance the capabilities of metamaterials further, additional dimensions have been incorporated, such as bianisotropy, material gain-loss contrast, and topological features of band structures [12–14], which all serve to lower the spatial symmetries of these materials. Recently, the field has seen significant progress in the ability to obtain tunable metamaterial parameters [15], which has enabled the introduction of time-varying material properties as a new means of controlling waves [16–19]. This is associated to the lowering of the continuous time-translational symmetry of metamaterials, and, as a result, a wide range of interesting phenomena have been proposed and are currently being actively explored, including magnet-free nonreciprocity [20–23], inverse prism [24], and effective frequency conversion [25–27]. For periodic temporal modulated systems, it can be generally classified as adiabatic, Floquet, and fast-driving regimes according to the size of the modulating frequency. In the adiabatic regime, in which the modulation frequency is much slower than the signal frequency, we can study the properties of the system with instantaneously varying external parameters. For example, it can be used to tune a topological edge state from one to another interface [28–30]. In the Floquet regime, in which the modulation and signal frequencies are in the same order, the band structure can be significantly modified to generate the so called "k-gaps" (rather than frequency gaps) [31], which can be useful for achieving parametric amplification, Floquet topological edge states, and nonreciprocal signal transport [32–34].

In this work, we are interested in the fast-driving regime, in which the modulation frequency is much higher than the signal frequency, termed a "temporal metamaterial" or "temporal effective medium," so that the whole medium can be described by effective medium parameters as if it is a static metamaterial [35]. The concept of a (spatial) effective medium is a powerful tool for macroscopically describing the response of metamaterials and for designing different optical and acoustic devices that require inhomogeneous profiles of effective media [36–39]. The temporal version of the effective medium theory, for instance, can be developed for "AB-stacking" time-varying metamaterials by modulating the permittivity of the medium over time. This temporal effective permittivity can be expressed as $1/\varepsilon_{\text{eff}} = \xi/\varepsilon_A + (1-\xi)/\varepsilon_B$, where ε_A and ε_B are the permittivities at time step A and time step B, with a duty cycle of ξ [35]. Additionally, by considering space and time modulation simultaneously in metamaterials, Huidobro *et al.* [40] have established an effective medium theory for traveling-wave modulations in the low-frequency limit. However, these theoretical works mainly focus on models of frequency-nondispersive materials with time-varying macroscopic material parameters. To incorporate the full capabilities of resonating metamaterial atoms, the frequency dispersion of time-varying metamaterial

*hwwu@aust.edu.cn
†jensenli@ust.hk

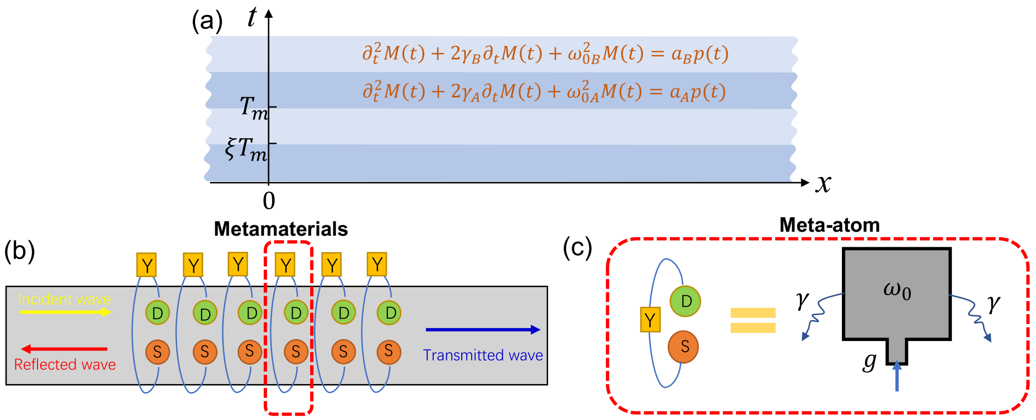

FIG. 1. Schematic diagram of the time-varying metamaterial. (a) The monopolar response switches between two different Lorentzian resonances with a modulation period of T_m. (b) Implementation using virtualized meta-atoms with period l. Each atom consists a pair of a detector (D) and a speaker (S) interconnected by an external microcontroller. Each microcontroller is programmed with an impulse response (Y) to mimic (c) a Helmholtz resonator with time-varying microscopic resonance strength g, resonating (radial) frequency ω_0 and linewidth γ. The microscopic resonance strength g is proportional to the resonance strength a in Eq. (3) by $a = 2cg/l$.

atoms can be included through dynamic Lorentzian media [41–43] and time-varying dipolar particles [44–46]. Furthermore, experimental demonstrations of the validity of the temporal effective medium concept can be achieved through the use of time-varying virtualized meta-atoms with resonating responses controlled by microcontrollers, which can serve as a testbed for various time-varying material physics [47]. Currently, the transition between effective medium formulas for frequency-dispersive and -nondispersive time-varying materials is not entirely clear, and the effective medium theory for considering different time-varying parameters in frequency dispersion has not been extensively explored.

In this work, we first show that temporal effective medium formulas for frequency-dispersive and -nondispersive material parameters can be different, and a phase transition between the two regimes can be captured by tuning the resonating frequency from small to values much larger than the modulation frequency. Additionally, we investigate the properties of a general time-varying, frequency-dispersive acoustic metamaterial in which not only the resonance strength, but also the resonant frequency, linewidth, or a combination of these parameters can be modulated over time. We establish a range of temporal effective medium formulas for these scenarios and validate them through the construction and experimentation of time-varying metamaterials using virtualized meta-atoms.

II. PHASE TRANSITION BETWEEN FREQUENCY-DISPERSIVE AND -NONDISPERSIVE TEMPORAL METAMATERIALS

We examine a one-dimensional (1D) (x), spatially homogeneous acoustic medium in which the material properties are periodically modulated in time (t) to generate a monopolar polarization $M(x, t)$ in the surrounding air. While the specific example used in this analysis pertains to airborne acoustic waves, the theoretical framework presented can be extended to other types of waves, such as electromagnetic waves. The wave equation in the case of airborne acoustics is given as

$$\partial_x p(x,t) + \rho_0 \partial_t v(x,t) = 0, \tag{1}$$

$$\partial_x v(x,t) + \beta_0 \partial_t (p(x,t) + M(x,t)) = 0, \tag{2}$$

where β_0 and ρ_0 are the compressibility and the density of air respectively. $p(x, t)$ represents the pressure field as a function of both x and t, while $v(x, t)$ is the velocity field. For simplicity, it is assumed that the metamaterial only possesses a single resonant frequency and responds to the pressure field through a Lorentzian-type model to generate only a monopolar response by

$$\partial_t^2 M(x,t) + 2\gamma(t)\partial_t M(x,t) + \omega_0^2(t) M(x,t) = a(t) p(x,t), \tag{3}$$

with $\omega_0(t)$ being the resonating (radial) frequency, $\gamma(t)$ being the resonating linewidth, and $a(t)$ being the resonance strength (in the unit of square frequency). The three resonance parameters (ω_0, γ, a) can vary in time, as depicted schematically in Fig. 1(a) with modulation period T_m. Each period of modulation consists of a duration defined by ξT_m (ξ is called the duty cycle), defining phase A, within which the frequency dispersion parameters are constants. The remaining time $(1-\xi)T_m$ within each period defines phase B. The density is always ρ_0, as the metamaterial only responds in a monopolar polarization. We note that this situation is established in analogy to a spatial effective medium in stacking two different stratified layers, but now in the time domain. In the electromagnetic case, it is well known that the effective medium formulas can be different for the two cases when the electric field is parallel or perpendicular to the layers. In the following, we show that the effective medium formulas can be different for modulating different resonance parameters. In this stage, we have assumed that the medium is invariant in x for ease of development of the theory. Later in the experimental stage, the medium will be constructed by placing a finite number of meta-atoms with a subwavelength periodicity l in x, as shown in Fig. 1(b), and the effective medium can be extracted by a scattering experiment at individual frequencies. We will adopt the virtualized meta-atom approach to construct the Lorentzian resonating response for each atom by connecting a pair of detectors and speakers [D and S, respectively, in Fig. 1(b)] through a microcontroller (Y) [27,47,48], mimicking Helmholtz resonators with time-varying resonating parameters, as shown in Fig. 1(c).

We now proceed to examine the case where only the resonance strength $a(t)$ is periodically modulated, while maintaining a constant temporal value of both ω_0 and γ. As we consider an infinite medium in the x direction, the propagation constant k along this direction remains unchanged across different time boundaries. In this scenario, Eqs. (1) to (3) can be rewritten ($\partial_x \to ik$) as

$$i\partial_t\psi = \hat{\omega}\psi,\ \hat{\omega} = \begin{pmatrix} 0 & \frac{k}{\beta_0} & 0 & i \\ \frac{k}{\rho_0} & 0 & 0 & 0 \\ 0 & 0 & 0 & -i \\ -ia & 0 & i\omega_0^2 & -i2\gamma \end{pmatrix}, \tag{4}$$

where the state vector is $\psi = (p, v, M, -\partial_t M)^T$. The propagation matrix, denoted as $\hat{\omega}$, switches between the two phases $\hat{\omega}_A$ and $\hat{\omega}_B$, corresponding to the resonance strengths a_A and a_B in the two phases. For the two static phases, by solving the harmonic from Eqs. (1)–(3) together with the constitutive relationship $\beta_0(p+M) = \beta p$, we obtain

$$\beta_{\mathrm{A/B}} = \beta_0\left(1 + \frac{a_{\mathrm{A/B}}}{\omega_0^2 - \omega^2 - 2i\gamma\omega}\right). \tag{5}$$

For the current case of time-varying medium, it is assumed that the modulation period is small enough to satisfy both ωT_m, $\omega_0 T_m \ll 1$, meaning that the modulating frequency is much higher than the signal frequency (or eigenfrequency of the mode in medium) and also much higher than the resonant frequency of the material. Under these conditions, the total transfer matrix can be approximated as $\exp(-i\hat{\omega}_{\mathrm{eff}} T_m)$, where $\hat{\omega}_{\mathrm{eff}} \cong \hat{\omega}_A\xi + \hat{\omega}_B(1-\xi)$ in the lowest order Taylor series expansion of the matrix exponential. This results in a time-averaged $a(t)$ [Eq. (4)]. By comparing this to Eq. (5), the effective medium formula for time-varying a and finite ω_0 can be obtained as

$$\beta_{\mathrm{eff}} = \xi\beta_A + (1-\xi)\beta_B. \tag{6}$$

This effective medium formula has been experimentally demonstrated in Ref. [47]. Interestingly, we also note that same effective medium formula results either we apply $a(t)$ to modulate $p(x,t)$ in Eq. (3) or alternatively to modulate the monopole sources in Eq. (2). On the other hand, in the case where the resonating (radial) frequency, denoted as ω_0, is extremely large, it is possible to approach a frequency-nondispersive time-varying medium. This is accomplished by expressing the modulation amplitude, denoted as $a_{\mathrm{A/B}} = \omega_0^2(\beta_{\mathrm{A/B}}/\beta_0 - 1)$. While the condition $\omega T_m \ll 1$ is still satisfied, the $\omega_0 T_m$ term is not small, thus preventing a direct use of the first-order Taylor series approximation. However, if the resonating linewidth, γ, is sufficiently large, it can effectively dampen the rapid oscillations of the monopolar polarization M triggered at each time boundary. By examining Eq. (4) in the limit of large ω_0, it can be proved that

$$i\partial_t(p+M) \cong \frac{k}{\beta_0}v, \quad i\partial_t v \cong \frac{k}{\rho_0}\frac{\beta_0}{\beta_{\mathrm{A/B}}}(p+M),$$

where $\beta_0(p+M) = \beta p$ and v are the continuity variables at each time boundary. It gives rise to the effective medium formula for time-varying modulation amplitude a at large ω_0:

$$1/\beta_{\mathrm{eff}} = \xi/\beta_A + (1-\xi)/\beta_B. \tag{7}$$

This effective medium formula has been adopted for a frequency-nondispersive time-varying medium [35].

For a general value of resonating frequency ω_0, regardless of whether it is small or large, we can use a numerical method to determine the eigenmode from Eq. (4) with a small positive eigenfrequency ω. Subsequently, the effective compressibility β_{eff} and the effective density ρ_{eff} can be calculated from the eigenmode using

$$\frac{\rho_{\mathrm{eff}}}{\rho_0} = \frac{k}{\omega\beta_0}\frac{v}{p+M},$$
$$\frac{\beta_{\mathrm{eff}}}{\beta_0} = \frac{k}{\omega\rho_0}\frac{p+M}{v}. \tag{8}$$

This approach is analogous to the method used to obtain the spatial effective medium, where the effective constitutive parameters are determined by the product and ratio of the refractive index and impedance from an eigenmode at a low frequency using the field variables in continuity (but now in time) [49]. This approach is employed for all numerical results presented in the following figures. Although we formulate the temporal effective medium in the acoustic 1D case, the extension to two dimensions or to an electromagnetic case are straightforward and are given in the Supplemental Material Appendix S1 [50]. Figure 2 illustrates the numerical results of β_{eff}, represented by the black solid line, when the resonating frequency $f_0 = \omega_0/(2\pi)$ is varied up to 25 kHz for a metamaterial with alternating modulation amplitude $a_A = 0$ and $a_B = \omega_0^2$ with a 50% duty cycle. The resonating linewidth is set as $\gamma = 0.2\omega_0$ and the modulation frequency is set as $1/T_m = 7.2$ kHz. The operational (eigen-) frequency is set at $\omega/(2\pi) = 1$ kHz. The red and blue dashed lines depict the two analytic effective medium formulas obtained by temporally averaging β [Eq. (6)] and temporally averaging $1/\beta$ [Eq. (7)], respectively. At low resonating frequencies, the results are in good agreement with the averaging of β. A phase transition occurs as the resonating frequency approaches the modulating frequency (7.2 kHz), and the results then align well with the averaging of $1/\beta$ as 1.33, as expected in the limit of a frequency-nondispersive time-varying medium with $\beta_A \cong 1$, $\beta_B \cong 2$. It should be noted that the effective density (not shown in the figure) is very close to the value of one, as the metamaterial only exhibits a resonating monopolar polarization response rather than a dipolar response.

III. EFFECTIVE MEDIUM FORMULA FOR MODULATING THE RESONATING FREQUENCY

After recognizing that different effective medium formulas can arise from different ways of setting up time-varying responses (between frequency-dispersive and -nondispersive

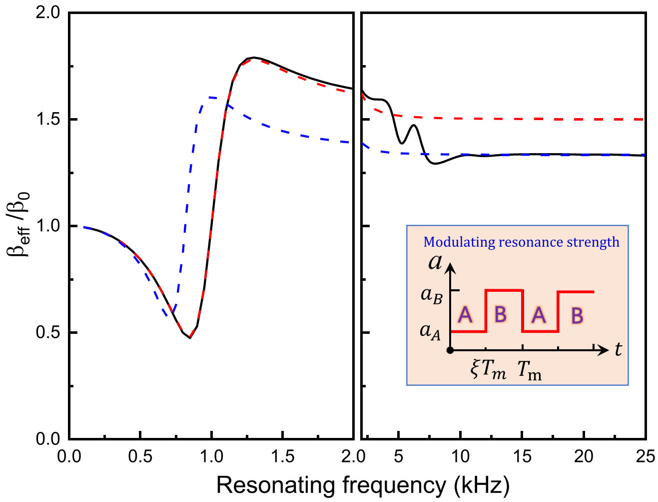

FIG. 2. Phase transition of temporal metamaterial from a frequency-dispersive to -nondispersive regime in increasing resonating frequency ω_0. Red and blue dashed lines correspond to the temporal average of compressibility (β) and bulk modulus ($1/\beta$), respectively. The black solid line is the effective compressibility (β_{eff}) from numerical calculations. The signal frequency, modulating frequency, and resonating linewidth are $\omega/(2\pi) = 1.0$ kHz, $1/T_m = 7.2$ kHz, and $\gamma = 0.2\omega_0$. The resonance strength of the temporal metamaterial is alternating in time between two static values, $a_A = 0$ and $a_B = \omega_0^2$, with duty cycle $\xi = 0.5$.

time-varying metamaterials [35,47]), we now discuss the case in which the resonating frequency ω_0 alternates between two finite values, $\omega_{0\text{A}}$ and $\omega_{0\text{B}}$, in phases A (with a duty cycle of η) and B, respectively. In this case, the resonance strength and linewidth, a and γ, are constant in time. The effective medium can be obtained by considering $\hat{\omega}_{\text{eff}} \cong \hat{\omega}_A \eta + \hat{\omega}_B(1-\eta)$. This translates to a time-averaged value of $\omega_0^2(t)$ and is equivalent to time-averaging $1/(\beta - \beta_0)$. The effective medium formula for a time-varying ω_0 becomes

$$\frac{1}{\beta_{\text{eff}} - \beta_0} = \frac{\eta}{\beta_A - \beta_0} + \frac{1-\eta}{\beta_B - \beta_0}, \tag{9}$$

where the static compressibility in each phase is

$$\beta_{\text{A/B}} = \beta_0 \left(1 + \frac{a}{\omega_{0\text{A/B}}^2 - \omega^2 - 2i\gamma\omega} \right). \tag{10}$$

As an example, we numerically calculate the effective medium parameters of a time-varying metamaterial by utilizing the eigenmode approach. The resonating frequencies of the metamaterial alternate between $\omega_{0\text{A}}/(2\pi) = 0.9$ kHz and $\omega_{0\text{B}}/(2\pi) = 1.1$ kHz. The resonance strength and linewidth are constant, with values of $a/(2\pi)^2 = 0.055\,\text{kHz}^2$ and $\gamma/(2\pi) = 15$ Hz, respectively. Additionally, the modulating frequency is set at $1/T_m =$ 7.2 kHz. To demonstrate the effectiveness of this approach, we plot the effective compressibilities β_{eff}, normalized to β_0, for three different duty

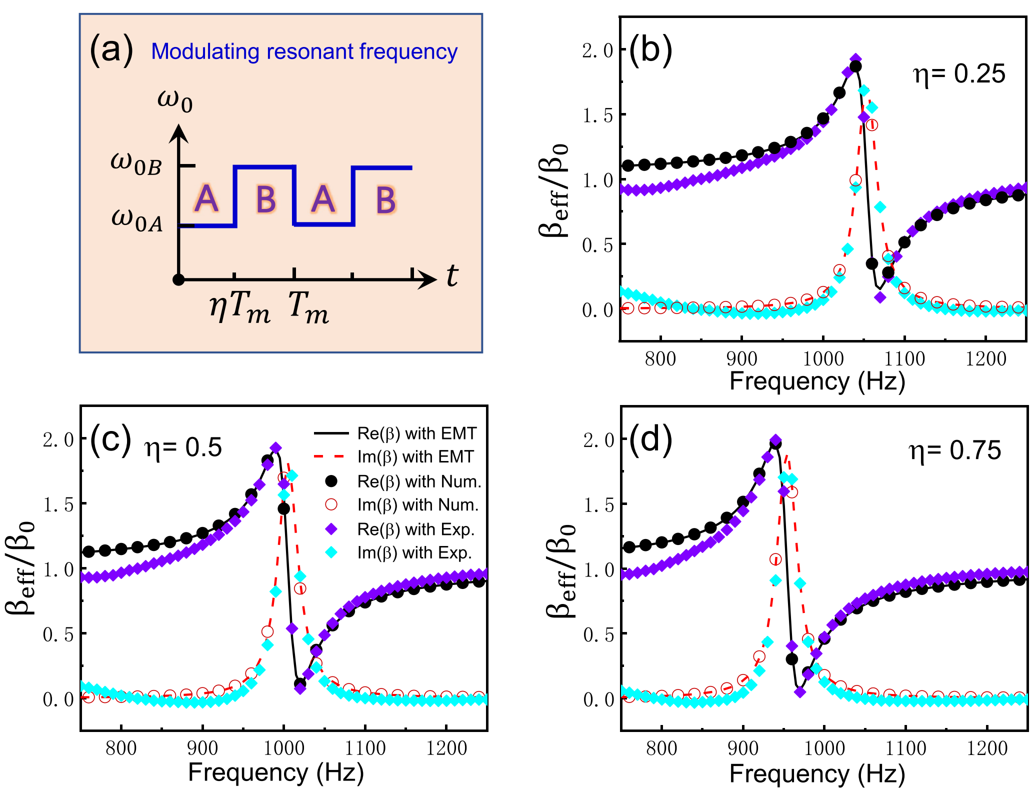

FIG. 3. (a) Schematic diagram for alternating resonating frequency between $\omega_{0\text{A}}$ and $\omega_{0\text{B}}$ with duty cycle η. The effective compressibility β_{eff} of the metamaterial, normalized by the one in air, is plotted for different duty cycles: (b) $\eta = 0.25$, (c) $\eta = 0.5$, and (d) $\eta = 0.75$. The solid and dashed lines show the real and imaginary parts, respectively, from the analytic formula Eq. (9), while the solid and hollow circles depict the numerical results from Eq. (8). The purple and cyan diamonds represent the experimental results extracted from scattering coefficients at individual frequencies. $\omega_{0\text{A}} = 2\pi \times 900$ Hz, $\omega_{0\text{B}} = 2\pi \times 1100$ Hz, $T_m = 139$ ms.

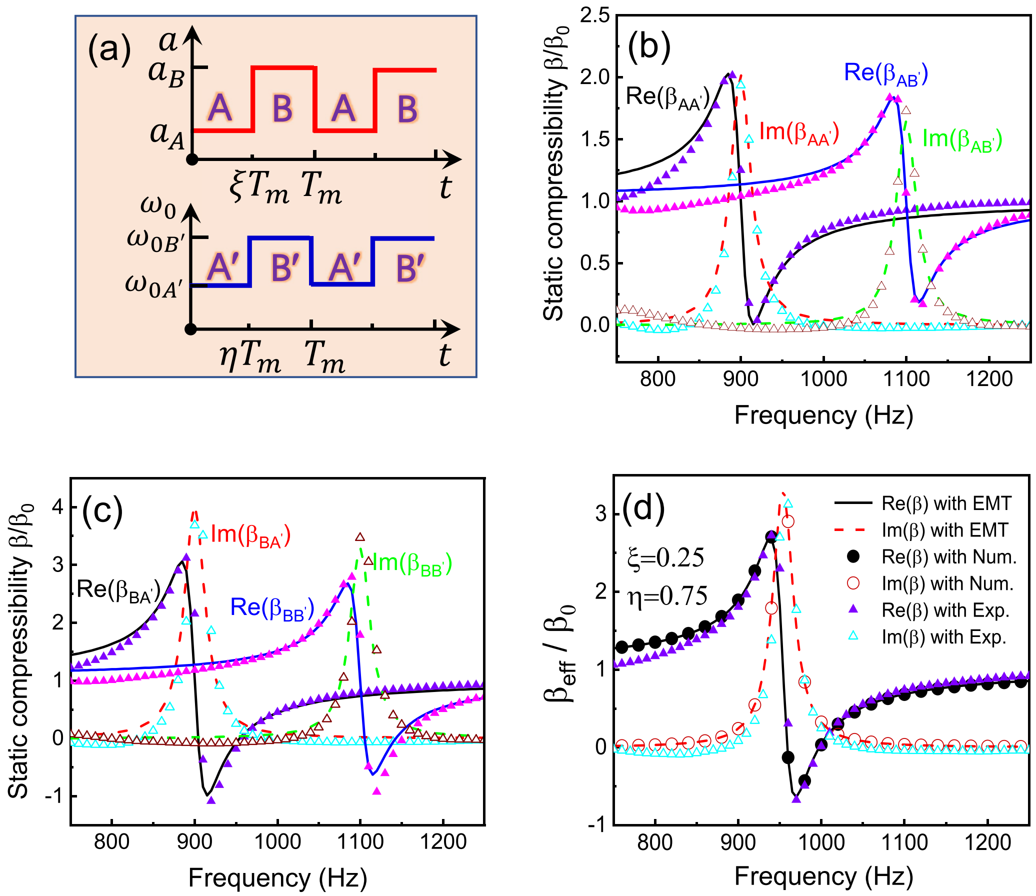

FIG. 4. (a) Schematic diagram of simultaneous time-varying resonance strength and frequency. (b) and (c) depict the four different combinations of static compressibilities—$\beta_{AA'}$, $\beta_{AB'}$, $\beta_{BA'}$, and $\beta_{BB'}$—as if the two modulations (phases A/B in modulating a and phases A′/B′ in modulating ω_0) can be shifted in time. The solid and dashed lines represent the theoretical results, and the solid and hollow triangles represent the experimental results. (d) shows the effective compressibility of time-varying metamaterial based on numerical, experimental results and the analytic results for the duty cycle pair $(\xi, \eta) = (0.25, 0.75)$ as circles, triangles, and lines, respectively.

cycles ($\eta = 0.25$, 0.5, and 0.75) in Figs. 3(b)–3(d). These results are represented by solid and hollow circle symbols for the real and imaginary parts, respectively, against the signal frequency $\omega/(2\pi)$. These numerical results match well with the effective medium formula obtained through time-averaging $1/(\beta - \beta_0)$ (black solid and red dashed lines for real and imaginary parts, respectively) with no notable differences.

We have experimentally implemented a time-varying metamaterial with alternating resonating frequencies. The metamaterial was constructed using virtualized meta-atoms in a 1D airborne acoustic waveguide in the x direction, as shown in Fig. 1(b). Each meta-atom was equipped with a microphone and a microcontroller that implemented a time-domain Lorentzian model to fire a speaker at the location of the same x. This process mimicked a Helmholtz resonator, as shown in Fig. 1(c), with a resonating frequency of ω_0, a linewidth of γ, and a microscopic resonance strength of g. The local structural model with a spatial periodicity of l between neighboring atoms was used to generate a static compressibility in the resonating form of Eq. (10) (see Supplemental Material Appendix S2 [50] for more details from the local to macroscopic model in relating g to a by $a = 2cg/l$). Note that in the experiment, the frequency spectrum of the speaker and the detector, and the electronic delay time of the microcontroller should be considered.

After experimentally setting up the static compressibilities in two phases separately according to the specified a, γ, and $\omega_{0\mathrm{A/B}}$, the two static media then alternated with each other with the three cases of duty cycles in the time domain. Complex transmission and reflection coefficients across the finite chain of atoms were then obtained experimentally at individual frequencies and were used to extract the effective medium parameters (details in Supplemental Material Appendix S3 [50], see also reference [51] therein), as shown by the purple and cyan diamonds for the real and imaginary parts of the effective compressibility in Figs. 3(b)–3(d). The experimental results agree well with the theoretical results, supporting time-averaging $1/(\beta - \beta_0)$. It is important to note that if β or $1/\beta$ is time-averaged, the results could show up in two resonances instead of one. Additionally, the same effective medium formula in averaging $1/(\beta - \beta_0)$ also works when the resonating linewidth γ is being modulated rather than the resonating frequency or strength, with additional results listed in the Supplemental Material Appendix S5 [50].

IV. EFFECTIVE MEDIUM FORMULA FOR SIMULTANEOUSLY MODULATING MULTIPLE PARAMETERS

To this point, we have presented results of modulation of a single resonance parameter. However, the programmability of our metamaterial allows for the simultaneous modulation of multiple parameters. In this case, we have implemented the alternating of both resonance strength and frequency. Specifically, we have used a duty cycle ξ to modulate the resonance strength between $a_A/(2\pi)^2 = 0.055\,\mathrm{kHz}^2$ and $a_B/(2\pi)^2 = 0.11\,\mathrm{kHz}^2$, while simultaneously using a duty cycle η to modulate the resonating frequency between $\omega_{0\mathrm{A}'}/(2\pi) = 0.9$ kHz and $\omega_{0\mathrm{B}'}/(2\pi) = 1.1\,\mathrm{kHz}$ within the same modulation period, as illustrated in Fig. 4(a). The resonating linewidth, $\gamma/(2\pi)$ was set as a constant of 15 Hz. The modulation frequency of $1/T_m = 7.2\,\mathrm{kHz}$ is much higher than the signal frequency, $\omega/(2\pi)$, thus the wave at individual signal frequencies is unable to "see" the fine details of the modulations. As a result, we expect the effective medium formula to be independent of the relative time shift between the two modulations. We have considered four different combinations: namely AA′, AB′, BA′, BB′, with definitions $\beta_{AA'} = 1 + a_A/\left(\omega_{0\mathrm{A}'}^2 - \omega^2 - 2i\gamma\omega\right)$, etc. These are plotted in Figs. 4(b) and 4(c) using lines for the analytic specifications and using triangles for the experimental realizations. The effective medium formula can be obtained through a cascaded procedure, first averaging $1/(\beta - \beta_0)$ for the ω_0 modulation, and then averaging β for the a modulation:

$$\begin{aligned}\frac{1}{\beta_A - \beta_0} &= \frac{\eta}{\beta_{AA'} - \beta_0} + \frac{1-\eta}{\beta_{AB'} - \beta_0},\\ \frac{1}{\beta_B - \beta_0} &= \frac{\eta}{\beta_{BA'} - \beta_0} + \frac{1-\eta}{\beta_{BB'} - \beta_0},\\ \beta_{\mathrm{eff}} &= \xi\beta_A + (1-\xi)\beta_B.\end{aligned} \tag{11}$$

Equivalently, the same effective medium formula can be obtained by first averaging β for the a modulation, and then averaging $1/(\beta - \beta_0)$ for the ω_0 modulation. The analytic results β_{eff} are illustrated as lines in Fig. 4(d) for a specific duty cycle pair of $(\xi,\ \eta) = (0.25, 0.75)$. To compare, the experimental results, extracted from the complex transmission and reflection coefficients, are represented by triangles, and the numerical results, obtained from numerical eigenmodes, are represented by circles. All results are in agreement with the analytic results as outlined in Eq. (11).

V. CONCLUSION

In summary, we have developed a temporal effective medium theory for metamaterials with time-varying frequency dispersion. Our findings indicate that the effective medium formula can change when different resonance parameters are modulated, or when the system shifts from a frequency-dispersive to a -nondispersive regime. These results were verified through experimental realizations using virtualized meta-atoms as a flexible platform. Additionally, we have outlined a cascaded procedure for obtaining the effective medium formula when multiple resonance parameters are modulated simultaneously. We anticipate that these findings will pave the way for future extension to more than one constitutive parameter, more resonances, and to other classical waves as well. Furthermore, this temporal effective medium theory will be useful in the design of compact topological and non-Hermitian devices based on temporal effective medium parameters.

ACKNOWLEDGMENTS

The work is supported by the Hong Kong Research Grants Council (Grants No. 16307522 and No. AoE/P-502/20) and the Croucher Foundation (CF23SC01). H.W.W. acknowledges support from the National Natural Science Foundation of China (Grant No. 11904008).

[1] D. R. Smith, W. J. Padilla, D. C. Vier, S. C. Nemat-Nasser, and S. Schultz, Phys. Rev. Lett. **84**, 4184 (2000).
[2] Z. Liu, X. Zhang, Y. Mao, Y. Y. Zhu, Z. Yang, C. T. Chan, and P. Sheng, Science **289**, 1734 (2000).
[3] N. Fang, D. Xi, J. Xu, M. Ambati, W. Srituravanich, C. Sun, and X. Zhang, Nat. Mater. **5**, 452 (2006).
[4] N. Yu, P. Genevet, M. A. Kats, F. Aieta, J. P. Tetienne, F. Capasso, and Z. Gaburro, Science **334**, 333 (2011).
[5] J. Valentine, S. Zhang, T. Zentgraf, E. Ulin-Avila, D. A. Genov, G. Bartal, and X. Zhang, Nature (London) **455**, 376 (2008).
[6] H. Zhu and F. Semperlotti, Phys. Rev. Lett. **117**, 034302 (2016).
[7] D. Schurig, J. J. Mock, B. J. Justice, S. A. Cummer, J. B. Pendry, A. F. Starr, and D. R. Smith, Science **314**, 977 (2006).
[8] T. Ergin, N. Stenger, P. Brenner, J. B. Pendry, and M. Wegener, Science **328**, 337 (2010).
[9] L. H. Gabrielli, J. Cardenas, C. B. Poitras, and M. Lipson, Nat. Photon. **3**, 461 (2009).
[10] C. Sheng, H. Liu, Y. Wang, S. N. Zhu, and D. A. Genov, Nat. Photon. **7**, 902 (2013).
[11] J. B. Pendry, Phys. Rev. Lett. **85**, 3966 (2000).
[12] R. Marqués, F. Medina, and R. Rafii-El-Idrissi, Phys. Rev. B **65**, 144440 (2002).
[13] L. Feng, Z. J. Wong, R. M. Ma, Y. Wang, and X. Zhang, Science **346**, 972 (2014).
[14] A. B. Khanikaev, S. Hossein Mousavi, W. K. Tse, M. Kargarian, A. H. MacDonald, and G. Shvets, Nat. Mater. **12**, 233 (2013).
[15] H. T. Chen, W. J. Padilla, J. M. Zide, A. C. Gossard, A. J. Taylor, and R. D. Averitt, Nature (London) **444**, 597 (2006).
[16] A. Rogov and E. Narimanov, ACS Photon. **5**, 2868 (2018).
[17] P. A. Huidobro, E. Galiffi, S. Guenneau, R. V. Craster, and J. B. Pendry, Proc. Nati. Acad. Sci. USA **116**, 24943 (2019).
[18] Y. Hadad, D. L. Sounas, and A. Alù, Phys. Rev. B **92**, 100304(R) (2015).
[19] C. Caloz and Z. L. Deck-Léger, IEEE Trans. Antennas Propag. **68**, 1569 (2019); **68**, 1583 (2019).
[20] Y. Wang, B. Yousefzadeh, H. Chen, H. Nassar, G. Huang, and C. Daraio, Phys. Rev. Lett. **121**, 194301 (2018).

[21] J. W. Zang, D. Correas-Serrano, J. T. S. Do, X. Liu, A. Alvarez-Melcon, and J. S. Gomez-Diaz, Phys. Rev. Appl. **11**, 054054 (2019).
[22] S. Taravati, Phys. Rev. Appl. **9**, 064012 (2018).
[23] J. Marconi, E. Riva, M. Di Ronco, G. Cazzulani, F. Braghin, and M. Ruzzene, Phys. Rev. Appl. **13**, 031001(R) (2020).
[24] A. Akbarzadeh, N. Chamanara, and C. Caloz, Opt. Lett. **43**, 3297 (2018).
[25] T. T. Koutserimpas and R. Fleury, Phys. Rev. Lett. **120**, 087401 (2018).
[26] K. Lee, J. Son, J. Park, B. Kang, W. Jeon, F. Rotermund, and B. Min, Nat. Photon. **12**, 765 (2018).
[27] X. Wen, X. Zhu, A. Fan, W. Y. Tam, J. Zhu, H. W. Wu, F. Lemoult, M. Fink, and J. Li, Commun. Phys. **5**, 18 (2022).
[28] Y. Xia, E. Riva, M. I. Rosa, G. Cazzulani, A. Erturk, F. Braghin, and M. Ruzzene, Phys. Rev. Lett. **126**, 095501 (2021).
[29] W. Cheng, E. Prodan, and C. Prodan, Phys. Rev. Lett. **125**, 224301 (2020).
[30] Y. X. Shen, L. S. Zeng, Z. G. Geng, D. G. Zhao, Y. G. Peng, and X. F. Zhu, Phys. Rev. Appl. **14**, 014043 (2020).
[31] J. R. Zurita-Sánchez, P. Halevi, and J. C. Cervantes-González, Phys. Rev. A **79**, 053821 (2009); G. Trainiti, Y. Xia, J. Marconi, G. Cazzulani, A. Erturk, and M. Ruzzene1, Phys. Rev. Lett. **122**, 124301 (2019).
[32] A. Cartella, T. F. Nova, M. Fechner, R. Merlin, and A. Cavalleri, Proc. Natl. Acad. Sci. USA **115**, 12148 (2018).
[33] R. Fleury, A. B. Khanikaev, and A. Alù, Nat. Commun. **7**, 11744 (2016).
[34] Z. Chen, Y. Peng, H. Li, J. Liu, Y. Ding, B. Liang, X. F. Zhu, Y. Lu, J. Cheng, and A. Alù, Sci. Adv. **7**, eabj1198 (2021).
[35] V. Pacheco-Peña and N. Engheta, Nanophotonics **9**, 379 (2020).
[36] R. Liu, T. J. Cui, D. Huang, B. Zhao, and D. R. Smith, Phys. Rev. E **76**, 026606 (2007).
[37] T. Koschny, M. Kafesaki, E. N. Economou, and C. M. Soukoulis, Phys. Rev. Lett. **93**, 107402 (2004).
[38] A. Alù, A. Salandrino, and N. Engheta, Opt. Express **14**, 1557 (2006).
[39] V. Fokin, M. Ambati, C. Sun, and X. Zhang, Phys. Rev. B **76**, 144302 (2007).
[40] P. A. Huidobro, M. G. Silveirinha, E. Galiffi, and J. B. Pendry, Phys. Rev. Appl. **16**, 014044 (2021).
[41] A. V. Maslov, A. A. Erykalin, and M. I. Bakunov, Phys. Rev. E **103**, 043207 (2021).
[42] M. I. Bakunov, A. V. Shirokova, and A. V. Maslov, Phys. Rev. B **104**, 035112 (2021).
[43] D. M. Solís, R. Kastner, and N. Engheta, Photon. Res. **9**, 1842 (2021).
[44] M. S. Mirmoosa, G. A. Ptitcyn, R. Fleury, and S. A. Tretyakov, Phys. Rev. A **102**, 013503 (2020).
[45] G. Ptitcyn, M. S. Mirmoosa, and S. A. Tretyakov, Phys. Rev. Res. **1**, 023014 (2019).
[46] M. S. Mirmoosa, T. T. Koutserimpas, G. A. Ptitcyn, S. A. Tretyakov, and R. Fleury, New J. Phys. **24**, 063004 (2022).
[47] X. Wen, X. Zhu, H. W. Wu, and J. Li, Phys. Rev. B **104**, L060304 (2021).
[48] C. Cho, X. Wen, N. Park, and J. Li, Nat. Commun. **11**, 251 (2020).
[49] J. Li and C. T. Chan, Phys. Rev. E **70**, 055602 (2004).
[50] See Supplemental Materials at http://link.aps.org/supplemental/10.1103/PhysRevB.108.104303 for more details on high-dimensional acoustic and electromagnetic time-varying systems, the discrete meta-atoms model, experimental realization, stability analysis, and additional results for time-modulating resonating linewidth.
[51] Y. Hao, Y. Shen, J. P. Groby, and J. Li, Wave Motion **112**, 102931 (2022).